Processing and Lysosomal Localization of a Glycoprotein Whose Secretion Is Transformation Stimulated

SUSANNAH GAL, MARK C. WILLINGHAM, and MICHAEL M. GOTTESMAN
Laboratory of Molecular Biology, National Cancer Institute, National Institutes of Health, Bethesda, Maryland 20205

ABSTRACT The major excreted protein (MEP) of transformed mouse fibroblasts is a mannose 6-phosphate–containing glycoprotein whose synthesis and secretion are increased in malignantly transformed 3T3 cells and whose synthesis is increased by treatment of 3T3 cells with tumor promoters or growth factors. When pulse-labeled extracts from Kirsten virus–transformed NIH 3T3 (KNIH) cells were immunoprecipitated using an antibody against secreted MEP, one cellular protein was immunoprecipitated that had the same molecular weight and tryptic peptide map as the secreted protein. Pulse-chase labeling experiments showed that 50–60% of this 39,000-mol-wt form was secreted in transformed cells. Of the 40–50% remaining, ~5% was processed into two lower molecular weight forms (29,000 and 20,000) which are sequestered within the cell. Similar processing of these proteins was observed in the nontransformed parent NIH 3T3 (NIH) cells. However, in NIH cells, much less of the synthesized MEP was secreted. Measurements of steady-state levels of these three forms of cellular MEP by Western blot immunolocalization revealed approximately fourfold more MEP in KNIH cells than in NIH cells as well as differences in the relative distribution of MEP forms in transformed and nontransformed cells. Subcellular fractionation of KNIH cells on a Percoll gradient demonstrated a distribution of total MEP similar to that of several lysosomal enzymes. The light lysosomal/Golgi peak from these gradients contained both the precursor 39,000-mol-wt form of MEP and the 20,000-mol-wt form, whereas the heavy lysosomal peak was enriched in the 20,000-mol-wt form. The distribution of MEP forms was found to be similar in NIH cells except that the 29,000-mol-wt form was also seen to be enriched in the heavy lysosomal peak. This biochemical localization of MEP was confirmed by immunolocalization with light and electron microscopy. These data support the hypothesis that MEP is a lysosomal protein that is secreted by transformed cells.

There are significant differences between the proteins secreted by fibroblastic cells with normal growth control and those secreted by cells that are malignantly transformed. The amounts of some secreted proteins, such as the extracellular matrix proteins collagen (1) and fibronectin (2), decrease, whereas the protease plasminogen activator (3) increases after transformation. It has been suggested that these protein changes may affect morphology and growth control (4) as well as invasiveness or metastasis of malignant fibroblasts.

We have been studying the secretion of a low molecular weight protein, MEP (major excreted protein),[1] by transformed murine fibroblasts. Increased MEP secretion was first observed in Kirsten sarcoma virus–transformed NIH 3T3 fibroblasts (KNIH cells). The secretion of this protein is increased 50- to 100-fold in these cells versus the NIH 3T3 (NIH) parent cell line (5). Various agents induce an increase in the synthesis and/or secretion of MEP: other tumor viruses (Harvey and Moloney sarcoma viruses and SV-40 [5]), phorbol ester tumor promoters (6, 7), and growth factors (platelet-derived growth factor [8] and fibroblast growth factor [9]). In mouse fibroblasts transformed virally or treated with tumor promoters, it has been shown that increased secretion of MEP is accompanied by a concomitant increase in the level of translatable MEP mRNA (6).

Although a function for MEP is not known, recent work has suggested that MEP has some properties in common with

[1] *Abbreviations used in this paper:* CHO, Chinese hamster ovary; KNIH, Kirsten virus–transformed NIH 3T3 (cells); MEP, major excreted protein; NIH, NIH 3T3 (cells).

the well-studied lysosomal enzymes. MEP is a phosphoglycoprotein (10) whose release can be stimulated in nontransformed Balb/c 3T3 cells (9) and Chinese hamster ovary cells by NH_4Cl (G. G. Sahagian, National Institute of Arthritis, Diabetes, Digestive and Kidney Diseases; personal communication)—properties shared by the lysosomal enzymes. Sahagian and Gottesman (11) have shown that the phosphate associated with this protein is present as mannose 6-phosphate. These residues allow binding of MEP to the phosphomannosyl receptor (11), which is required for targeting of lysosomal enzymes to lysosomes in cultured fibroblasts (12). These data suggest that MEP is either an unusual lysosomal protein which is secreted in transformed cells or a mannose 6-phosphate–containing secretory protein. In this study, we find that the intracellular processing and the subcellular localization of MEP indicate it is a lysosomal protein. We find that MEP is processed within both nontransformed and transformed cells into two lower molecular weight forms. Gradient fractionation of subcellular organelles demonstrates the presence of nascent and processed MEP in the Golgi region of the gradient while the lower molecular weight forms of MEP are found in the lysosomal peak. The localization of MEP in the Golgi complex and lysosomes has been confirmed by indirect immunofluorescence and electron microscopic localization.

MATERIALS AND METHODS

Cell Culture: NIH and KNIH cells obtained from C. Scher (Harvard Medical School) were maintained at 37°C in 5% CO_2 in Dulbecco's modified Eagle's medium (HEM Laboratories, Rockville, MD) supplemented with penicillin (50 U/ml), streptomycin (50 μg/ml), and 10% calf serum (Colorado Serum Co., Denver, CO). Cells were trypsinized with 0.25% trypsin (Microbiological Associates, Walkersville, MD) in Tris-dextrose buffer (National Institutes of Health [NIH] media unit). NIH cells were trypsinized with 0.25% trypsin and 0.2 mM EDTA in Tris-dextrose buffer.

Labeling and Immunoprecipitation of Labeled Proteins: Monolayer cultures were labeled with either [^{35}S]methionine or [^{35}S]-cysteine (20–50 μCi/ml) in Dulbecco-Vogt medium lacking the appropriate amino acid (NIH media unit). For pulse-chase experiments, the labeling medium was replaced with normal growth medium to begin the chase period. Cells were lysed on the dishes with SDS-Buffer A (0.154 M NaCl, 0.05 M Tris-HCl, pH 7.4, 0.5% Nonidet P-40, 0.05% SDS), and lysates were clarified by centrifugation at 12,000 *g* for 2 min. Immunoprecipitation of labeled protein was performed using *Staphylococcus aureus* as previously described (19). The pellets were treated with SDS dissociation buffer (see below) and boiled before electrophoresis.

SDS PAGE: Samples dissolved in SDS dissociation buffer (2.5% SDS, 10% glycerol, 5% 2-mercaptoethanol, and 0.0625 M Tris-HCl, pH 6.8) were boiled 3 min and clarified by centrifugation at 12,000 *g* for 2 min. Electrophoresis was performed as described by Laemmli (13) except that the separating gel contained 10% glycerol and 0.5% linear acrylamide (14). For the determination of molecular weight, SDS polyacrylamide gels were cast without glycerol or linear acrylamide at three different acrylamide concentrations (10, 12.5, and 15%). Stained gels were prepared for fluorography after destaining as described by Bonner and Laskey (15). The gels were exposed to preflashed X-Omat AR film (Kodak) at −70°C; radioactivity was quantitated by densitometry on a Joyce-Loebel 3CS microdensitometer (Joyce-Loebel, Gateshead, England) and the peak areas were measured with an electronic planimeter (Numonics Corp., Lansdale, PA) or by weighing excised peaks. ^{14}C-Molecular weight markers (Amersham Corp., Arlington Heights, IL) for the gels were lysozyme (14,000 mol wt), carbonic anhydrase (30,000), ovalbumin (46,000), BSA (69,000), phosphorylase *b* (92,500), and myosin (200,000).

Tryptic Peptide Maps: Gel bands of proteins of interest were excised and two-dimensional tryptic peptide maps were performed as described by Shih et al. (16). The chromatography plates were dipped in 0.4% 2,5-diphenyloxazole in naphthalene (17), allowed to cool, and exposed to x-ray film at −70°C.

Percoll Gradients: Cells were grown to 70–80% confluence in roller bottles (750 cm^2), rinsed with PBS, and scraped off with a spatula. The cells were pelleted and resuspended in gradient buffer (0.25 M sucrose, 20 mM HEPES, pH 7.0, 0.02% azide) at 1 × 10^7 cells/ml. The method of Rome et al. (18) was used to obtain a postnuclear supernate. This method involves nitrogen cavitation to swell the cells and Dounce homogenization to lyse them. Whole cells and nuclei were pelleted by centrifugation at 600 *g* for 15 min. 5 ml of this supernate was loaded on 25 ml of 30% Percoll (Pharmacia Fine Chemicals, Piscataway, NJ) in gradient buffer over a 2-ml saturated sucrose cushion. The Percoll gradient was formed at 18,500 rpm (27,500 *g*) in a Sorvall TV-850 vertical rotor (E. I. DuPont de Nemours & Co., Inc., Sorvall Instruments Div., Newton, CT) for 1 h and 1-ml fractions were collected from the top. Density marker beads (Pharmacia Inc.) were used to estimate the density profile of the gradient.

Enzymatic and Protein Assays: Lysosomal enzyme activities were determined by using the 4-methyl umbelliferyl substrates (1 mM) in 0.1 M Na acetate buffer, pH 4.4, in the presence of 0.1% Triton (18). Fluorescence was measured on an Aminco-Bowman spectrofluorometer (Amicon Corp., Danvers, MA) with excitation beam set at 365 nm and emission beam at 455 nm. Results are given in arbitrary fluorescence units. We assayed galactosyl transferase by measuring the radioactivity transferred to *N*-acetyl glucosamine from UDP-[^{3}H]galactose (12 Ci/mmol; New England Nuclear, Boston, MA) in 10 mM Tris, 5 mM $MnCl_2$, 1% Triton at 37°C (19). The nucleotide sugar was added at 4 × 10^5 cpm per 0.5-ml reaction, and *N*-acetyl glucosamine was at a concentration of 15 mM. We separated the precursor and product on a Dowex column (Dowex-1-chloride, 4% cross-linkage, 50–100 dry mesh; Sigma Chemical Co., St. Louis, MO) by rinsing the reaction mixture through the column with water and determined blank values by doing duplicate assays without *N*-acetyl glucosamine. Protein was analyzed by the method of Bradford (20) using ovalbumin as the standard.

Western Blot Analysis: Proteins were electrophoretically transferred to nitrocellulose paper from an SDS gel as described by Towbin et al. (21) in transfer buffer (25 mM Tris, 92 mM glycine, pH 8.3, 20% methanol). We used a Bio-Rad Trans-Blot chamber (Bio-Rad Laboratories, Richmond, CA) at 200 mA for 3 h. MEP was immunolocalized using the technique of Cabral et al. (22). The first antibody was affinity purified on a MEP-Sepharose column by the method of Cabral et al. (23). The second antibody was ^{125}I-Protein A (Amersham Corp.) used at a concentration of 5–10 μCi in 30 ml of incubation buffer. The nitrocellulose paper with the immunolocalized MEP proteins was blotted dry and exposed to x-ray film. The radioactivity associated with the nitrocellulose paper was quantitated in the same manner as for the gels.

Immunofluorescence and Electron Microscopy: NIH and KNIH cells grown in 35-mm culture dishes were fixed for immunofluorescence with 3.7% formaldehyde in PBS for 10 min at 23°C. The cells were then treated with 0.1% Triton X-100 in PBS for 3 min at 23°C, washed in PBS, and incubated in the "EGS" diluent (24) composed of 0.1% saponin, 4 mg/ml normal goat globulin, and 1 mM EGTA-PBS (sap-NGG-PBS) for 10 min. Affinity-purified rabbit anti-MEP was then added at 50 μg/ml in sap-NGG-PBS for 15 min at 23°C. The cells were washed in PBS and then incubated in affinity-purified goat anti-rabbit IgG conjugated to rhodamine (Jackson ImmunoResearch) in sap-NGG-PBS for an additional 15 min. After being washed in PBS, the cells were mounted under a circular (No. 1) coverslip in glycerol, viewed with a Zeiss standard microscope equipped with a 63X, oil (NA 1.4) planapochromat objective with rhodamine epifluorescence optics, and photographed on Kodak Tri-X film which was developed in Diafine. For electron microscopic immunocytochemistry, NIH and KNIH cells were fixed and processed using the EGS procedure (24) with 0.2% glutaraldehyde in the primary fixative. MEP was localized with affinity-purified rabbit anti-MEP at 50 μg/ml in sap-NGG-PBS using the ferritin bridge sequence (24). After antibody incubations and postfixation in glutaraldehyde and OsO_4, the dishes were dehydrated with ethanol and embedded in Epon 812. Thin sections were counterstained with lead citrate and bismuth subnitrate as previously described (24) and viewed at 50 kV. Controls included the use of an equivalent amount of normal rabbit globulin in the first step of the ferritin bridge or immunofluorescence sequence, and they were uniformly negative.

RESULTS

MEP Is Processed into Two Lower Molecular Weight Forms Intracellularly

Immunoprecipitation of MEP from extracts of cells labeled with [^{35}S]methionine for >1 h reveals three major forms of this protein in KNIH (11) and NIH cells. These proteins have molecular weights of 39,000, 29,000, and 20,000 as determined by their migration in SDS polyacrylamide gels using several gel concentrations and BSA, ovalbumin, carbonic anhydrase, and lysozyme as protein standards. The molecular

weights reported here are slightly different from those published earlier (5, 11). Previous molecular weight values were based on behavior in gels that contained glycerol and linear acrylamide, which may have affected our estimation of molecular weight.

We performed pulse-chase experiments labeling with [^{35}S]-methionine and [^{35}S]cysteine to evaluate the possible precursor–product relationship of these three forms of MEP. When [^{35}S]cysteine was used as a metabolic label, a clear sequential appearance of the three major forms of MEP was observed in both cell types. Fig. 1 shows the pulse-chase analysis of [^{35}S]-cysteine-labeled MEP in KNIH cells and Fig. 2 shows a similar experiment with NIH cells. In the experiment with the KNIH cells, ~52% of the [^{35}S]cysteine-containing MEP was secreted and 45% was unaccounted for by the autoradiographic band densities by the end of the experiment (Fig. 1 *a*). In both this experiment with [^{35}S]cysteine labeling and the one with [^{35}S]-methionine labeling (data not shown), there was a rapid loss of labeled MEP immediately after synthesis (within 30 min of chase) prior to either secretion or processing, which accounted for 35 and 40% of [^{35}S]cysteine- and [^{35}S]methionine-labeled MEP, respectively. This loss of label could represent processing of MEP in these cells to non-immunoreactive forms, early degradation of nascent protein, or sequestering of protein in a cell compartment not extractable by detergent. The likely precursor–product relationship of these three forms was clearly demonstrated here with the sequential appearance of the 29,000-mol-wt form and finally the relatively stable 20,000-mol-wt form. [^{35}S]Cysteine pulse-chase labeling of NIH cells (Fig. 2) also demonstrated processing of the 39,000-mol-wt MEP protein similar to the 29,000- and 20,000-mol-wt cellular forms. The high molecular weight bands (~200,000) are fibronectin bands that bind nonspecifically to *S. aureus*. By using the graphic representation of the cysteine pulse-chase labeling in both cell types (Figs. 1 *c* and 2 *c*), approximate rates of interconversion of the MEP forms can be assessed. NIH cells processed the two lower molecular weight proteins more slowly. The 29,000-mol-wt form appeared at the same rate but it took 75 min for half of the 29,000-mol-wt form to be processed to the 20,000-mol-wt form in NIH cells whereas it took only ~45 min in KNIH cells. This was reflected in a longer time to reach maximal levels of the 20,000-mol-wt form in nontransformed cells (6 h vs. 3 h in KNIH cells). The time to degrade half of the

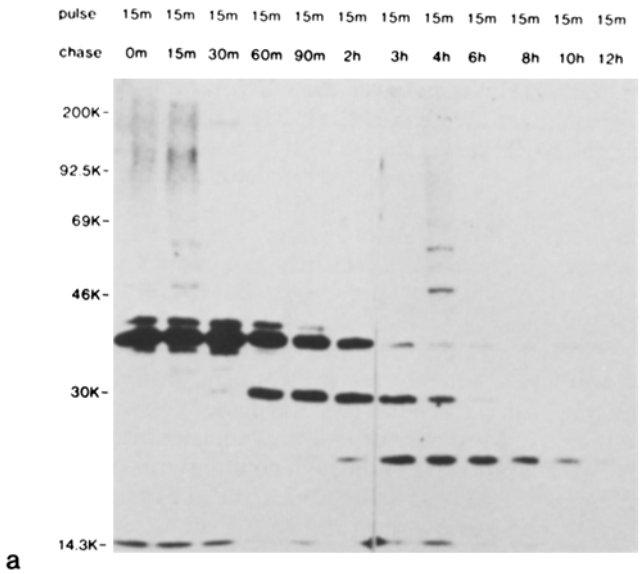

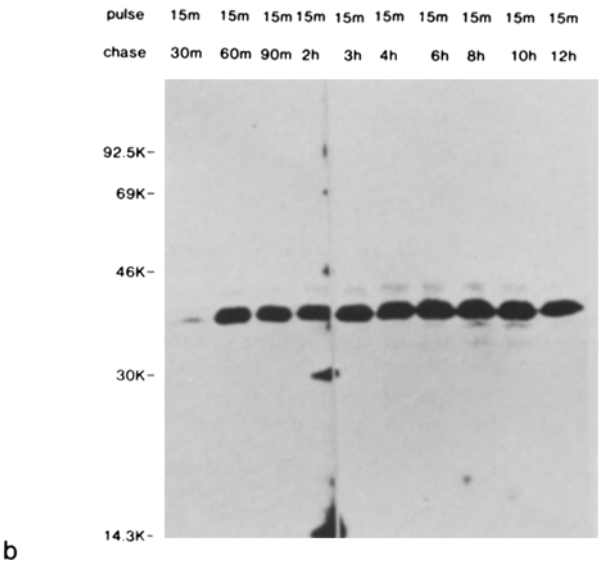

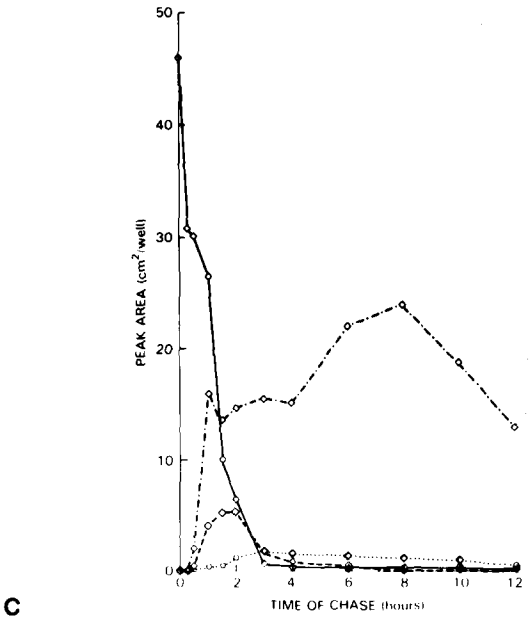

FIGURE 1 Kinetics of processing [^{35}S]cysteine-labeled MEP in KNIH cells. (*a*) Fluorogram of a 10% acrylamide gel of radiolabeled immunoprecipitates from KNIH cell extracts. The cells were plated in six-well multiwell dishes at 10^5 cells/well 2 d before the experiment, pulse-labeled for 15 min at 37°C, and then incubated in chase medium for the indicated times. Approximately 10^5 trichloroacetic acid–precipitable counts from the pulse cell sample (50% of total incorporated counts) and equivalent volumes of the other cell samples were incubated with the antibody. (*b*) Fluorogram of a 10% acrylamide gel of radiolabeled immunoprecipitates from KNIH cell media. The cells were treated as described above and 10% of the total medium volume was immunoprecipitated. Molecular weights in *a* and *b* are in thousands. (*c*) Plot of autoradiographic band density (as peak area) versus time of chase. The plot shows the presence of the various forms of MEP: cellular 39,000-mol-wt MEP (◇–◇–◇), secreted 39,000-mol-wt MEP (◇.–.◇.–.◇), cellular 29,000-mol-wt MEP (◇– –◇– –◇), and cellular 20,000-mol-wt MEP (○....○....○).

lowest molecular weight form of MEP was ~8 h in KNIH cells whereas in NIH cells we observed little or no degradation of this protein during the time of chase (compare Figs. 1 *c* and 2 *c*). We did not observe the early large loss of total MEP-incorporated radioactivity with the NIH cells that we observed with the KNIH cells.

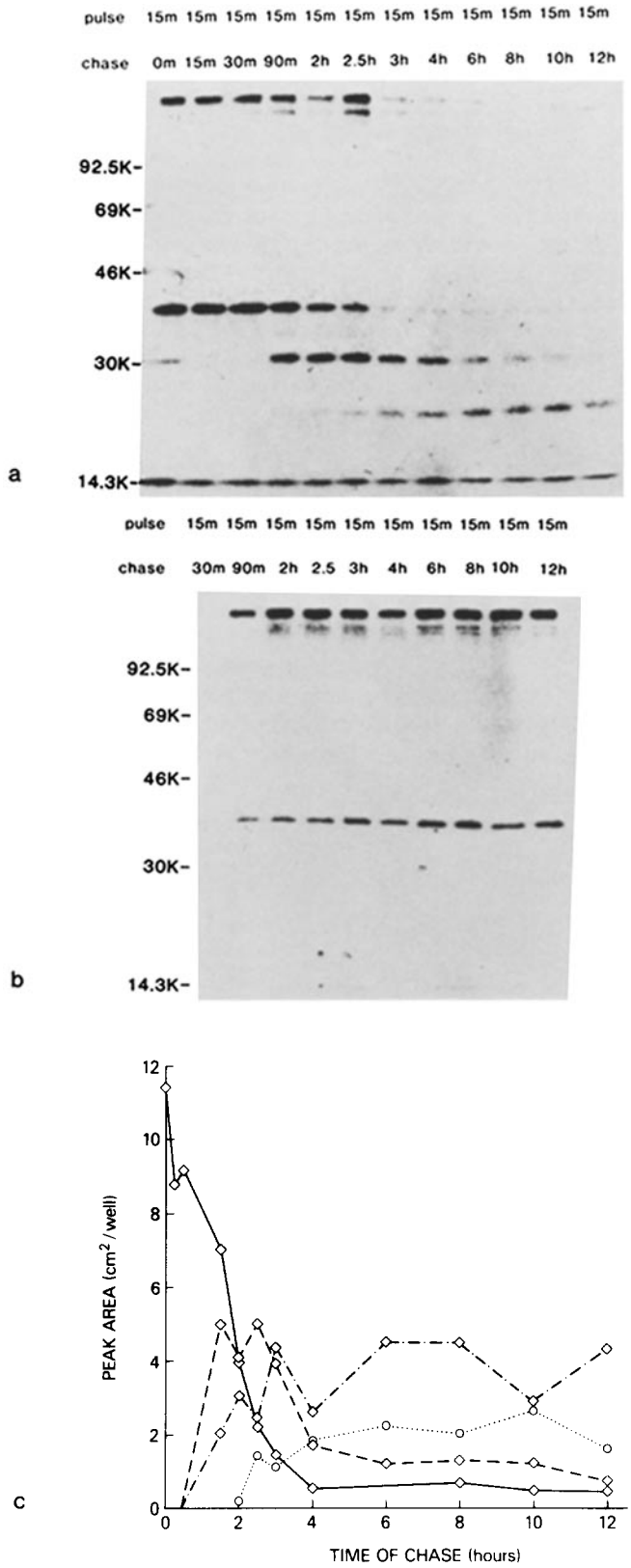

In the [^{35}S]methionine pulse-chase labeling experiments (data not shown), we found that ~60% of the label initially incorporated into the 39,000-mol-wt MEP was secreted into the medium in KNIH cells compared with only 5% in NIH cells. Some of the labeled MEP remaining within the cell was converted to the two lower molecular weight species, and some of the original methionine label was not recovered as immunoprecipitable protein in both cell types.

Tryptic peptide maps of the three intracellular forms of MEP (Fig. 3) demonstrate that the earliest form of MEP seen within the cells has the same peptide map as that previously published for secreted MEP (10), while the two lower molecular weight forms contain only a few of the methionine-containing peptides seen in the secreted form. [^{35}S]methionine-labeled maps of both nascent (Fig. 3 *a*) and secreted MEP (10) show four major labeled peptides in the lower right of the map with many spots to the left and above these spots. The two lower molecular weight forms have many peptides in common with each other and contain a subset of the peptides seen in the 39,000-mol-wt dalton protein. As seen in Fig. 3, *b* and *c*, the 29,000- and 20,000-mol-wt forms of MEP are missing three of the heavily labeled spots seen in the map of the 39,000-mol-wt precursor. Presumably, those [^{35}S]methionine-containing peptides are lost in the processing that takes place to form the 29,000- and 20,000-mol-wt proteins. When tryptic peptides from the 39,000-mol-wt cellular form and the 29,000-mol-wt form were mixed in ratios of 1:1 and 1:3 (not shown), we found no major additional spots compared with those in the map of the 39,000-mol-wt protein alone. These results indicate that the 29,000- and 20,000-mol-wt forms of MEP are probably cleavage products of the 39,000-mol-wt MEP and that a methionine-rich portion of the MEP molecule is removed by processing. The tryptic peptide map of the 39,000-mol-wt cellular MEP from NIH cells (Fig. 3 *d*) is very similar to the KNIH cell protein. This indicates no gross differences in the structures of these proteins in NIH cells compared with KNIH cells.

Short pulses with [^{35}S]cysteine were performed to try to detect a precursor of the 39,000-mol-wt form of MEP in KNIH cells. No immunoprecipitable protein with higher or lower molecular weight was observed in pulses as short as 30 s (Fig. 4). The band of slightly higher molecular weight (42,000) observed in many of the immunoprecipitations (e.g., Fig. 1) probably does not represent a precursor but is more

FIGURE 2 Kinetics of processing [^{35}S]cysteine-labeled MEP in NIH cells. (*a*) Fluorogram of a 10% acrylamide gel of radiolabeled immunoprecipitates from NIH cell extracts. The cells were plated in six-well multiwell dishes at 2 × 10^4 cells/well 4 d before the experiment, pulse-labeled for 15 min at 37°C, and then incubated in chase medium for the indicated times. Approximately 5 × 10^4 trichloroacetic acid-precipitable counts from the pulse cell sample (30% of total incorporated counts) and equivalent volumes of the other cell samples were incubated with the antibody. (*b*) Fluorogram of a 10% acrylamide gel of radiolabeled immunoprecipitates from NIH cell media. The cells were treated as described above and 30% of the total medium volume was immunoprecipitated. Molecular weights in *a* and *b* are in thousands. (*c*) Plot of autoradiographic band density (as peak area) versus time of chase. The plot shows the presence of the various forms of MEP: cellular 39,000-mol-wt MEP (◇–◇–◇), secreted 39,000-mol-wt MEP (◇–·–◇–·–◇), cellular 29,000-mol-wt MEP (◇– –◇– –◇), and cellular 20,000-mol-wt MEP (○···○···○).

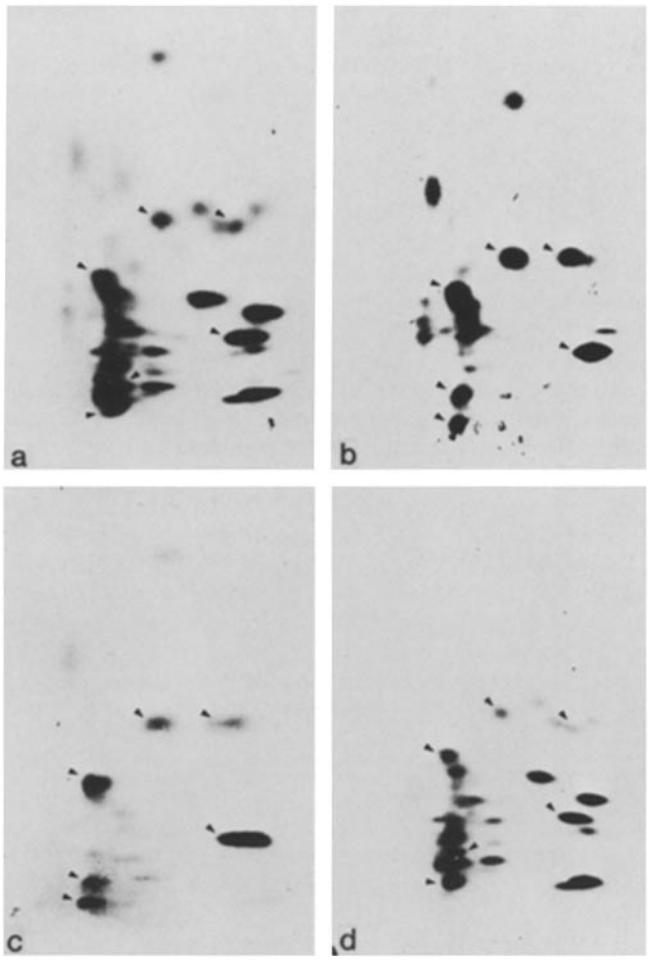

FIGURE 3 Two-dimensional tryptic peptide analysis of [^{35}S]methionine-labeled peptides of various forms of MEP: cellular 39,000-mol-wt MEP (*a*), cellular 29,000-mol-wt MEP (*b*), cellular 20,000-mol-wt MEP (*c*) from KNIH cells, and cellular 39,000-mol-wt MEP from NIH cells (*d*). The samples were electrophoresed in the horizontal direction with the cathode to the right and then chromatographed vertically. The arrowheads indicate corresponding peptides in the four maps.

likely a differently glycosylated form. This protein has the same tryptic map as the 39,000-mol-wt form (10) and is present in the same ratio to the amount of 39,000-mol-wt protein throughout the short pulse labeling with [^{35}S]cysteine. This form of MEP represents only a small fraction of the steady-state concentration of cellular MEP, as seen in the Western blot (Fig. 5, lane *a*).

Steady-state levels of MEP proteins within KNIH and NIH cells were quantitated by analysis of Western blot patterns in total cell extracts (Fig. 5). As the assay is not strictly quantitative with respect to the protein bound, the amount of antibody binding to each of the MEP forms can only be used to approximate the amount of the form present. From this type of analysis, we observed a very different distribution of MEP forms in the two cell types. KNIH cells were found to contain primarily the 20,000- and 39,000-mol-wt proteins and relatively little of the 29,000-mol-wt form (Fig. 5, lanes *a–d*). Pulse-chase labeling showed that the middle form is more stable in NIH cells, and we observed a higher relative amount of this protein in these cells by Western analysis (Fig. 5, lanes *e–h*). Total MEP levels within NIH cells were approximately one fourth that in KNIH cells for the same number of cells or amount of cell protein.

Subcellular Localization of MEP by Density Gradient Fractionation

Disrupted cells were fractionated on a self-forming Percoll gradient, and the fractions were analyzed for β-galactosidase activity and galactosyl transferase activity to localize lysosomes and Golgi apparatus, respectively (KNIH cells in Fig. 6*a* and NIH cells in Fig. 7*a*). We found three areas of β-galactosidase activity in both gradients, the least dense of which can be attributed to soluble enzyme from broken organelles (18). Similar profiles were obtained for both cell types with two other lysosomal enzymes, α-glucuronidase and α-galactosidase (data not shown). We observed a single peak of galactosyl transferase activity which co-sedimented with the lighter lysosomal enzyme activity in the gradients from KNIH and NIH cells. We observed a relative distribution of the lysosomal enzyme marker β-galactosidase in KNIH cells that was different from that observed in NIH cells. KNIH cells show a majority of intact organelle enzymatic activity in the light lysosomal or Golgi peak while most of the activity in NIH cells sediments with the heavy lysosomal peak (compare Figs. 6*a* and 7*a*). Approximately 70% of the total intact β-galactosidase activity is associated with the light lysosomal peak in KNIH cells while only 40% is observed to sediment in that region in NIH cells. This difference is also seen in the distribution of the activities of the two other lysosomal enzymes (data not shown).

Samples from gradient fractions were electrophoresed on SDS polyacrylamide denaturing gels, transferred to nitrocellulose paper, and localized with an affinity-purified antibody

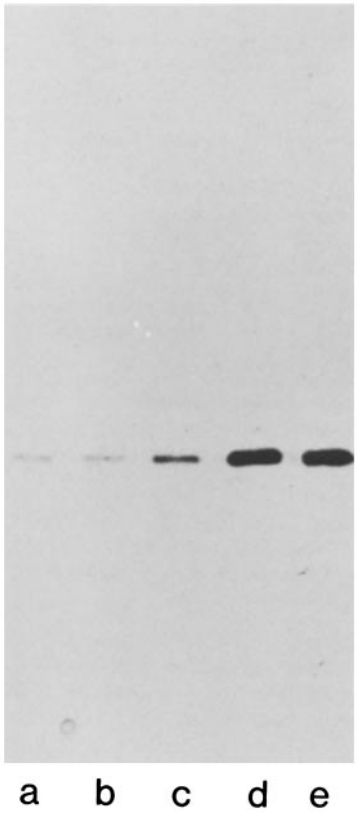

FIGURE 4 Kinetics of the appearance of 39,000-mol-wt cellular MEP. Immunoprecipitates of [^{35}S]-cysteine - radiolabeled KNIH cell extracts were electrophoresed in a 10% acrylamide gel. A fluorogram is shown. The cells were pulsed with labeling medium for 30 s (lane *a*), 1 min (lane *b*), 2 min (lane *c*), 5 min (lane *d*), and 15 min (lane *e*). Approximately 3 × 10^4 trichloroacetic acid–precipitable counts from the 15-min pulse sample (50% of the sample) and equal volumes of the other extracts were incubated with the antibody.

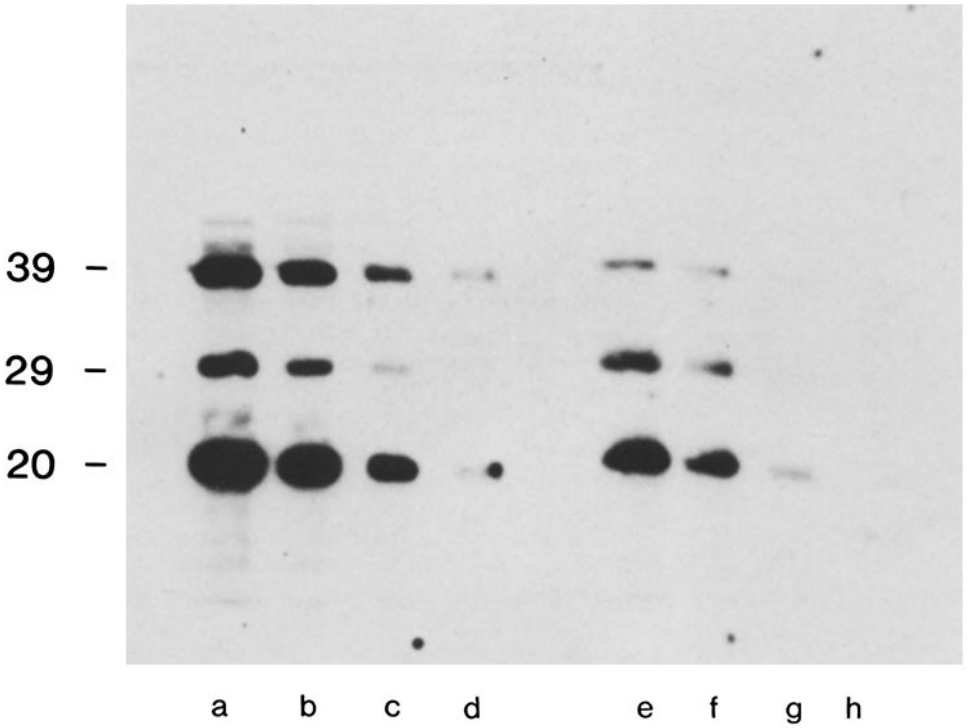

FIGURE 5 Western blot localization of MEP forms in KNIH and NIH cells. This autoradiogram shows the steady-state distribution of MEP forms in KNIH (lanes *a–d*) and NIH cells (lanes *e–h*). Total protein loaded: lane *a* (6×10^4 cells) and lane e (7×10^4 cells), 20 μg; lanes *b* and *f*, 10 μg; lanes c and *g*, 5 μg; lanes *d* and *h*, 2.5 μg. 39, 39,000; 29, 29,000; 20, 20,000.

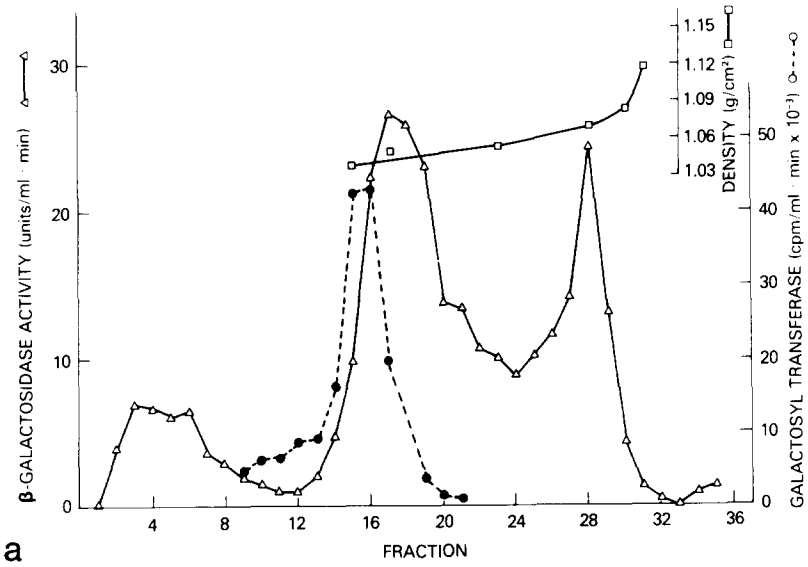

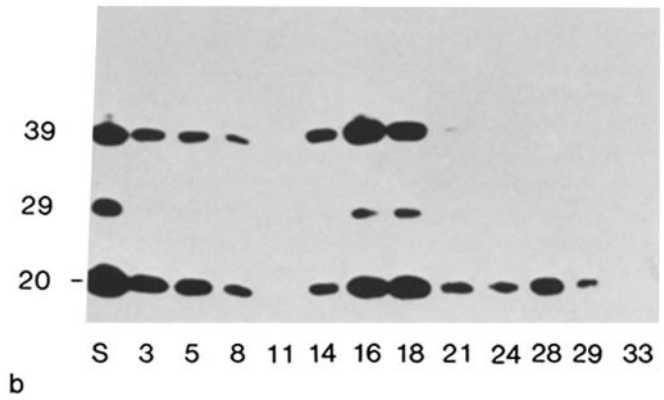

FIGURE 6 Percoll gradient of KNIH cell extracts. (*a*) The enzymatic and density profile of the gradient. Lysosomes were localized by β-galactosidase activity and Golgi elements by galactosyl transferase activity. Density marker beads (Pharmacia Fine Chemicals) were used to determine the density profile of the gradient. (*b*) Western blot localization of MEP in the gradient fractions. Approximately 25 μl of each fraction (labeled by fraction number) and the loading sample (*S*) were electrophoresed on a 10% acrylamide gel, electrolytically transferred to nitrocellulose, and localized with anti-MEP antibody as described in Materials and Methods. The molecular weight of the bands is indicated at the side. 39, 39,000; 29, 29,000; 20, 20,000.

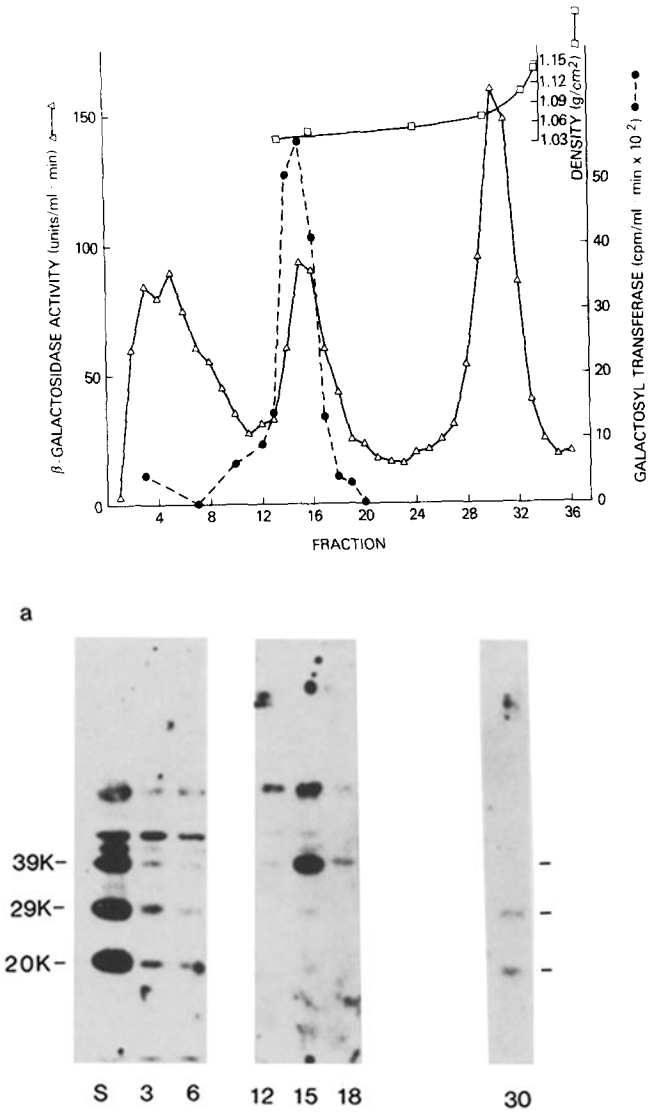

FIGURE 7 Percoll gradient of NIH cell extracts. (a) The enzymatic and density profile of the gradient. Lysosomes were localized by β-galactosidase activity and Golgi elements by galactosyl transferase activity. Density marker beads (Pharmacia, Inc.) were used to determine the density profile of the gradient. (b) Western blot localization of MEP in the gradient fractions. Approximately 25 μl of each fraction (labeled by fraction number) and the loading sample (S) were electrophoresed on a 10% acrylamide gel, electrolytically transferred to nitrocellulose, and localized with anti-MEP antibody as described in Materials and Methods. The molecular weight of the bands is indicated at the side in thousands.

against the secreted form of MEP (KNIH cells in Fig. 6*b* and NIH cells in Fig. 7*b*). This technique measures steady-state levels of the various forms of MEP since we use ^{125}I-protein A to localize anti-MEP antibody. MEP appeared in three peaks on both gradients at the same densities as β-galactosidase activity, the lysosomal marker. We also observed a difference in the localization of the various forms of MEP. The lighter lysosomal/Golgi peak was enriched in the 39,000- and 20,000-mol-wt forms of MEP in the gradients using both KNIH and NIH cells, whereas the heavier peak showed enrichment in the lowest molecular weight forms. The 29,000-mol-wt protein is a minor component of the steady-state cellular pool of MEP in KNIH cells. In NIH cells, a greater proportion of the MEP was in the 29,000-mol-wt form and it was definitely enriched in the heavy lysosomal peak as was the 20,000-mol-wt protein. The background on the NIH Western blot was much greater than on a similar blot for KNIH cells because these cells have much lower amounts of MEP. The band above the MEP bands in Fig. 7*b* (~60,000-mol-wt) represents nonspecific localization of ^{125}I-protein A.

Immunofluorescence and Electron Microscopic Localization of MEP

Fig. 8, *A* and *B* shows the immunofluorescence localization of MEP in NIH (Fig. 8*A*) and KNIH (Fig. 8*B*) cells. The predominant pattern in NIH cells appears as punctate intracellular spots compatible with the distribution of lysosomes, in addition to a bright cytoplasmic fluorescence slightly concentrated in the perinuclear region. The pattern in KNIH cells shows the punctate arrangement, but this is partially obscured by a brighter cytoplasmic localization particularly concentrated in an eccentric location in the perinuclear area compatible with parts of the Golgi system. By electron microscopic immunocytochemistry (Fig. 8, *C–F*), MEP in NIH cells was found to be most concentrated in mature lysosomes (Fig. 8*E*), with a smaller concentration in the trans elements of the Golgi stacks (Fig. 8*C*). A similar pattern was seen in KNIH cells, but the concentrations were greater (Fig. 8, *D* and *F*). In addition, lower concentrations of label were seen in the nuclear envelope, endoplasmic reticulum, and the transreticular elements of the Golgi apparatus (not shown). The overall amount of MEP detected inside NIH cells was less than that seen in KNIH cells, consistent with biochemical measurements. An unexplained low level of specific background localization was also seen in both cell types diffusely distributed in the extramembranous cytoplasm. The same distribution of ferritin granules was seen using an affinity-purified antibody prepared from antiserum from a different rabbit. Normal globulin controls showed very low nonspecific levels of localization (data not shown).

DISCUSSION

The major excreted protein of transformed mouse cells (MEP) is a 39,000-mol-wt phosphoglycoprotein whose synthesis is also enhanced by growth factors and tumor promoters. We have found that within mouse cells there are several forms of MEP that cross-react with a polyclonal antibody made against the protein excreted by transformed cells. One major form of MEP has the same molecular weight as the secreted form and the same tryptic map, and thus is presumed to be part of the intracellular pool of MEP either not secreted or just prior to secretion. Very short pulse labeling (30 s) shows no immunoreactive precursor form of molecular weight >39,000 prior to the appearance of the 39,000-mol-wt protein. Since the primary translation product of MEP is immunoreactive and has a molecular weight lower by several thousand than MEP (6), it seems reasonable to assume from these data that glycosylation of MEP in living cells is a co-translational event. Two other cellular forms of MEP have lower molecular weights and similar but simpler tryptic maps. The pulse-chase labeling experiments described in this paper indicate that these proteins are processed forms of cellular MEP.

Both transformed and nontransformed mouse cells used in this study contain MEP as precursor and processed forms. By

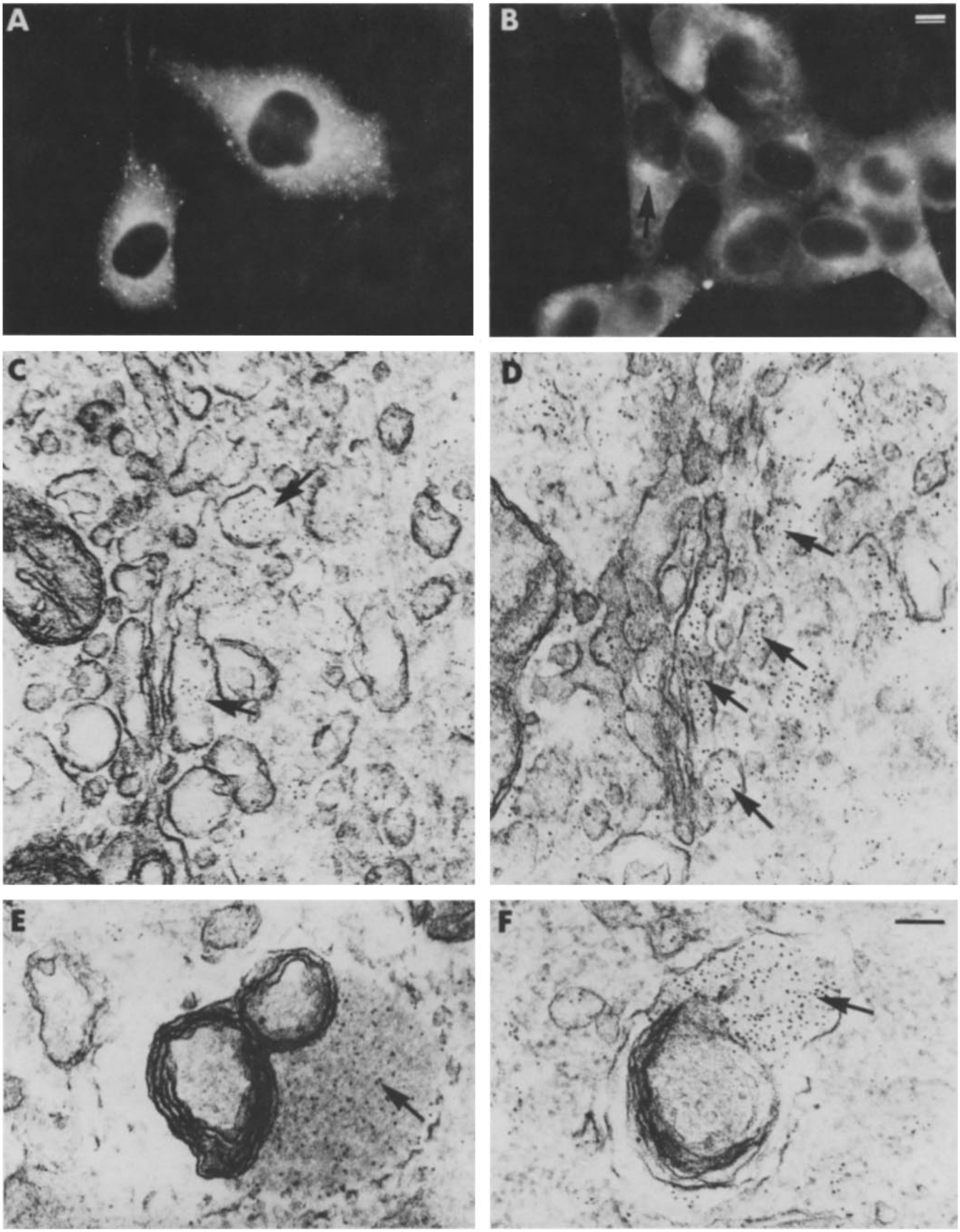

FIGURE 8 Immunocytochemical localization of MEP. NIH (*A*, *C*, and *E*) and KNIH (*B*, *D*, and *F*) cells were fixed and processed as described in Materials and Methods. MEP was localized using immunofluorescence (*A* and *B*) or electron microscopic immunocytochemistry using the EGS and ferritin bridge procedures (*C–F*). The immunofluorescence pattern in NIH cells (*A*) is predominantly punctate (lysosomal) with some perinuclear concentration; the pattern in KNIH cells (*B*) is brighter with some punctate elements, but the main pattern is a perinuclear eccentric location (arrow) consistent with elements of the Golgi complex. The electron microscopic pattern in both cell types shows *trans*-Golgi concentration (arrows), which is more concentrated in KNIH cells (*D*) than in NIH cells (*C*). Both cell types show high concentrations of labeling in lysosomes (arrows, *E* and *F*) Bars, 10 μm (*A* and *B*); 0.1 μm (*C–F*). (*A* and *B*) × 577; (*C–F*) × 90,000.

tryptic peptide analysis, the precursor forms in both cell types appear very similar (compare Fig. 3, *a* and *d*). In both cell types, the immunoreactive proteins can be localized to the same organelles as lysosomal proteins with biochemical and microscopic assays. Yet, there are major differences between the transformed and nontransformed cells: (*a*) KNIH cells synthesize 50-fold more total MEP than NIH cells and secrete 50–60% of the 39,000-mol-wt protein made vs. 5–28% in NIH cells: (*b*) there is four- to fivefold more MEP in KNIH cells than in NIH cells and the relative distribution of the various forms of MEP is also different; and (*c*) in KNIH cells, 70% of lysosomal enzyme activity sediments in the light lysosomal/Golgi fraction whereas the majority (~60%) of the activity for NIH cells sediments in the heavy lysosomal peak. The distribution of lysosomal enzyme activity seen with CHO (25) cells is similar to the distribution for NIH cells. These data suggest that there is a general difference in the way KNIH cells handle lysosomal enzymes compared with NIH cells as well as specific differences in how MEP is regulated in these cell types.

The data presented here and in a previous paper (11) are consistent with the view that MEP is a lysosomal protein. We previously showed (11) that the secreted MEP from KNIH cells contains the mannose 6-phosphate recognition marker and binds to the mannose 6-phosphate receptor that is involved in the shuttling of lysosomal enzymes in the cell (12). In this study, we have shown by two different methods, Percoll gradient fractionation and immunofluorescence and electron microscopic localization, that cellular MEP localizes to lysosomes and the Golgi apparatus in the same manner as lysosomal enzymes. The putative precursor form of MEP (39,000 mol wt) is found in the light lysosomal peak but not in the denser one, while the two processed forms (29,000 and 20,00 mol wt) are found in both the heavy and light lysosomal fractions. This is consistent with the localization of other precursor and processed forms of lysosomal enzymes such as cathepsin D and β-hexosaminidase (26). These data do not allow us to determine whether processing of MEP precedes its appearance in the lysosomal fraction or occurs after migration to the lysosomes.

We considered the possibility that the MEP "processing" in KNIH cells observed in this work might simply be the degradation of the secreted form following its reuptake via mannose 6-phosphate receptors and delivery to lysosomes. This possibility is ruled out by the observation (data not shown) that the lower molecular weight forms of MEP appear in cells labeled in medium that contains 5 mM mannose 6-phosphate which blocks the binding of MEP to the mannose 6-phosphate receptor (11).

The work described above suggests that MEP in nontransformed cells is a fairly typical lysosomal protein. However, there are two observations that are not entirely consistent with MEP being a typical lysosomal protein. Despite the ability of MEP to bind to purified mannose 6-phosphate receptor, it is not taken up with 100% efficiency by CHO cells (11). This result is in contrast to that found with β-galactosidase from KNIH cells whose secretion can be stimulated by NH_4Cl treatment. This β-galactosidase is efficiently endocytosed by CHO cells and processed normally (11). Second, 50–60% of the 39,000-mol-wt form of MEP is secreted by KNIH cells even in the absence of NH_4Cl. Thus, it appears that a fraction of MEP is selectively segregated from the lysosomal enzyme pool and secreted in these transformed cells despite the binding of this protein to the phosphomannosyl receptor (11).

Intracellularly packaged proteins such as lysosomal enzymes and secreted proteins are synthesized in rough endoplasmic reticulum, processed in the Golgi stacks, and segregated in vesicles that bud off of the Golgi complex. At some point along this pathway, the two types of proteins must diverge since their eventual destinations, lysosomes or secretory vesicles, are morphologically and biochemically distinct. Little is known about the mechanism or signal for this segregation. Mannose 6-phosphate is believed to be the marker for proteins destined to reside in lysosomes; however in the case of MEP this signal may not be sufficient or may not be properly displayed on the surface of the protein, or another signal may disrupt this segregation in KNIH cells. Uteroferrin, a secreted lysosomal protein, has a "covered" mannose 6-phosphate which may explain the routing of the secreted form to the cell surface (27). There is also evidence from several laboratories that the mannose 6-phosphate receptor system may not be sufficient for delivery of acid hydrolases to lysosomes in some cell types. Patients with I-cell disease lack the enzyme required to form the mannose 6-phosphate moiety on lysosomal proteins (28, 29). As a consequence, fibroblasts from these patients secrete their acid hydrolases (30). But other types of cells in the same patients, such as hepatocytes, Kupffer cells, and leukocytes, contain nearly normal levels of lysosomal enzymes (31, 32). Work by Gabel et al. (33) with murine macrophage mutants and by Robbins and Myerowitz (34) with CHO cell mutants with reduced levels of the mannose 6-phosphate receptor show that these mutant cells contain significant levels of acid hydrolases within their lysosomes. An alteration in a routing mechanism other than the one requiring mannose 6-phosphate may explain the secretion of MEP in KNIH cells. By studying a protein that has properties of both secreted and lysosomal proteins, such as MEP, more may be revealed about the mechanism of this segregation.

The correlation of MEP synthesis and secretion with transformation is another intriguing aspect of our study. Lysosomes contain proteins with activities that could be involved in local invasion of tumors, metastasis, or tumor related syndromes. These lysosomal enzyme activities include phospholipases (35), neuraminidases (36), hyaluronidase (37), collagenase (38), and various proteases (39–41). Sloan and coworkers (42) have found that the lysosomal protease cathepsin B may be correlated wtih transformation. These workers observed a relationship between metastatic potential in B16 melanoma cells and cathepsin B activity in tumor homogenates. We are continuing to search for an enzymatic activity associated with MEP and are now cognizant of the possibility that the activity may reside only in the processed forms of this protein.

We thank Drs. April R. Robbins, G. Gary Sahagian, Robert B. Dickson, and Paul J. Doherty for helpful discussions and critical comments on this manuscript. We also thank Raymond L. Steinberg for his photographic assistance.

Received for publication 12 July 1984, and in revised form 15 October 1984.

REFERENCES

1. Green, H., G. J. Todaro, and B. Golderg. 1966. Collagen synthesis in fibroblasts transformed by oncogenic viruses. *Nature (Lond.)*. 209:916–917.
2. Yamada, K. M., and K. Olden. 1978. Fibronectins—adhesive glycoproteins of cell

surface and blood. *Nature (Lond.)*. 275:179–184.
3. Unkeless, J. C., A. Tobia, L. Ossowski, J. P. Quigley, D. B. Rifkin, and E. Reich. 1973. An enzymatic function associated with transformation of fibroblasts by oncogenic viruses. I. Chick embryo fibroblast cultures transformed by avian RNA tumor viruses. *J. Exp. Med.* 137:85–112.
4. Pastan, I., and M. Willingham. 1978. Cellular transformation and the 'morphologic phenotype' of transformed cells. *Nature (Lond.)*. 274:645–650.
5. Gottesman, M. M. 1978. Transformation-dependent secretion of a low molecular weight protein by murine fibroblasts. *Proc. Natl. Acad. Sci. USA*. 75:2767–2771.
6. Cabral, F., M. M. Gottesman, and S. H. Yuspa. 1981. Induction of specific protein synthesis by phorbol esters in mouse epidermal cell culture. *Cancer Res.* 41:2025–2031.
7. Gottesman, M. M., and M. E. Sobel. 1980. Tumor promoter and Kirsten sarcoma virus increase the synthesis of a secreted glycoprotein by regulating levels of translatable mRNA. *Cell*. 19:449–455.
8. Scher, C. D., S. L. Hendrickson, A. P. Whipple, M. M. Gottesman, and W. J. Pledger. 1982. Constitutive synthesis by a tumorigenic cell line of proteins modulated by platelet-derived growth factor. *Cold Spring Harbor Conf. Cell Prolif.* Vol. 9 (Book A):289–303.
9. Nilsen-Hamilton, M., R. T. Hamilton, W. R. Allen, and S. L. Massoglia. 1981. Stimulation of the release of two glycoproteins from mouse 3T3 cells by growth factors and by agents that increase lysosomal pH. *Biochem. Biophys. Res. Commun.* 101:411–417.
10. Gottesman, M. M., and F. Cabral. 1981. Purification and characterization of a transformation-dependent protein secreted by cultured murine fibroblasts. *Biochemistry*. 20:1659–1665.
11. Sahagian, G. G., and M. M. Gottesman. 1982. The predominant secreted protein of transformed murine fibroblasts carries the lysosomal mannose 6-phosphate recognition marker. *J. Biol. Chem.* 257:11145–11150.
12. Gonzalez-Noriega, A., J. H. Grubb, V. Talkad, and W. S. Sly. 1980. Chloroquine inhibits lysosomal enzyme pinocytosis and enhances lysosomal enzyme secretion by impairing receptor recycling. *J. Cell Biol.* 85:839–852.
13. Laemmli, U. K. 1970. Cleavage of structural proteins during the assembly of the head of bacteriophage T4. *Nature (Lond.)*. 227:680–685.
14. Cabral, F., and G. Schatz. 1979. High resolution one- and two-dimensional electrophoretic analysis of mitochondrial membrane peptides. *Methods Enzymol.* 56:602–613.
15. Bonner, W. M., and R. A. Laskey. 1974. A film detection method for tritium labeled proteins and nucleic acids in polyacrylamide gels. *Eur. J. Biochem.* 46:83–88.
16. Shih, T. Y., D. R. Williams, M. O. Weeks, J. M. Maryak, W. C. Vass, and E. M. Scolnick. 1978. Comparison of the genomic organization of Kirsten and Harvey sarcoma viruses. *J. Virol.* 27:45–55.
17. Bonner, W. M., and J. D. Stedtman. 1978. Efficient fluorography of ^{3}H and ^{14}C on thin layers. *Anal. Biochem.* 89:247–256.
18. Rome, L. H., A. J. Garvin, M. M. Allietta, and E. F. Neufeld. 1979. Two species of lysosomal organelles in cultured human fibroblasts. *Cell*. 17:143–153.
19. Fleischer, B., S. Fleischer, and H. Ozawa. 1969. Isolation and characterization of Golgi membranes from bovine liver. *J. Cell Biol.* 43:59–79.
20. Bradford, M. M. 1976. A rapid and sensitive method for the quantitation of microgram quantities of protein utilizing the principle of protein-dye binding. *Anal. Biochem.* 72:248–254.
21. Towbin, A., J. Staehelin, and J. Gordon. 1979. Electrophoretic transfer of proteins from polyacrylamide gels to nitrocellulose sheets: procedure and some applications. *Proc. Natl. Acad. Sci. USA*. 76:4350–4354.
22. Cabral, F., I. Abraham, and M. M. Gottesman. 1982. Revertants of a Chinese hamster ovary cell mutant with an altered β-tubulin: evidence that the altered tubulin confers both Colcemid resistance and temperature sensitivity on the cell. *Mol. Cell. Biol.* 2:720–729.
23. Cabral, F., M. C. Willingham, and M. M. Gottesman. 1980. Ultrastructural localization to 10nm filaments of an insoluble 58K protein in cultured fibroblasts. *J. Histochem. Cytochem.* 28:653–662.
24. Willingham, M. C. 1980. Electron microscopic immunocytochemical localization of intracellular antigens in cultured cells: the EGS and ferritin bridge procedures. *Histochem. J.* 12:419–434.
25. Robbins, A. R., S. S. Peng, and J. L. Marshall. 1983. Mutant Chinese hamster ovary cells pleiotropically defective in receptor-mediated endocytosis. *J. Cell Biol.* 96:1064–1071.
26. Hasilik, A., L. H. Rome, and E. F. Neufeld. 1979. Processing of lysosomal enzymes in human skin fibroblasts. *Fed. Proc.* 38:467.
27. Baumbach, G. A., P. T. K. Saunders, F. W. Bazer, and R. M. Roberts. 1984. Uteroferrin has N-asparagine-linked high-mannose-type oligosaccharides that contain mannose 6-phosphate. *Proc. Natl. Acad. Sci. USA*. 81:2985–2989.
28. Hasilik, A., A. Waheed, and K. von Figura. 1981. Enzymatic phosphorylation of lysosomal enzymes in the presence of UDP-N-acetylglucosamine. Absence of the activity in I-cell fibroblasts. *Biochem. Biophys. Res. Commun.* 98:761–767.
29. Reitman, M. L., A. Varki, and S. Kornfeld. 1981. Fibroblasts from patients with I-cell disease and pseudo-Hurler polydystrophy are deficient in uridine 5′-diphosphate-N-acetylglucosamine; Glycoprotein *N*-acetylglucosaminylphosphotransferase activity. *J. Clin. Invest.* 67:1574–1579.
30. McKusick, V. A., E. F. Neufeld, and T. E. Kelly. 1978. The mucopolysaccharide storage diseases. *In* The Metabolic Basis of Inherited Disease. J. B. Stanbury, J. B. Wyngaarden, and D. S. Frederickson, editors. McGraw Hill, New York. Fourth ed. 1282–1307.
31. Owada, M., and E. F. Neufeld. 1981. Is there a mechanism for introducing acid hydrolases into liver lysosomes that is independent of mannose 6-phosphate recognition? Evidence from I-cell disease. *Biochem. Biophys. Res. Commun.* 105:814–820.
32. Waheed, A., R. Pohlmann, A. Hasilik, K. von Figura, A. van Elsen, and J. G. Leroy. 1982. Deficiency of UDP-N-acetylglucosamine: lysosomal enzyme N-acetylglucosamine-1-phosphotransferase in organs of I-cell patients. *Biochem. Biophys. Res. Commun.* 105:1052–1058.
33. Goldberg, D. E., and S. Kornfeld. 1983. Identification and characterization of cells deficient in the mannose 6-phosphate receptor: evidence for an alternate pathway for lysosomal enzyme targeting. *Proc. Natl. Acad. Sci. USA*. 80:775–779.
34. Robbins, A. R., and R. Myerowitz. 1981. The mannose 6-phosphate receptor of Chinese Hamster Ovary cells—compartmentalization of acid hydrolases in mutants with altered receptors. *J. Biol. Chem.* 256:10623–10627.
35. Waite, M., G. L. Scherphot, F. M. B. Boshouwers, and L. L. M. Van Deenen. 1969. Differentiation of phospholipases A in mitochondria and lysosomes of rat liver. *J. Lipid Res.* 10:411–420.
36. Horvat, A., and O. Touster. 1968. On the lysosomal occurrence and the properties of the neuraminidase of rat liver and of Ehrlich ascites tumor cells. *J. Biol. Chem.* 243:4380–4390.
37. Vaes, G. 1967. Hyaluronidase activity in lysosomes of bone tissue. *Biochem. J.* 103:802–804.
38. Wynn, C. H. 1967. Solubilization of insoluble collagens by rat liver lysosomes. *Nature (Lond.)*. 215:1191–1192.
39. McDonald, J. K., T. J. Reilly, B. B. Zeitman, and S. Ellis. 1968. Dipeptidyl arylamidase II of the pituitary. *J. Biol. Chem.* 243:2028–2037.
40. Bowers, W. E., and C. deDuve. 1967. Lysosomes in lymphoid tissue. II. Intracellular distribution of acid hydrolases. *J. Cell Biol.* 32:339–348.
41. Snellman, O. 1969. Cathepsin B, the lysosomal thiol proteinase of calf liver. *Biochem. J.* 114:673–678.
42. Sloan, B. F., J. R. Dunn, and K. V. Honn. 1981. Lysosomal cathepsin B: correlation with metastic potential. *Science (Wash. DC)*. 212:1151–1154.